Unsteady, viscous, circular flow

Part 2. The cylinder of finite radius

By MERWIN SIBULKIN

Convair Scientific Research Laboratory, San Diego

(Received 27 February 1961, and in revised form 7 August 1961)

The problem considered is that of the two-dimensional motion of the fluid in a cylinder of finite radius after the outer portion of the fluid is given an initial uniform velocity. The primary purpose of the investigation is the study of the changes in the energy distribution in the fluid as the initial motion decays. The appropriate flow equations are developed and then approximated by finite-difference equations. Numerical solutions of these equations are presented, and the energy-transfer processes are discussed in some detail. During the early stages of the flow, it is found that the spatial distribution of energy depends strongly on the Prandtl number. During the later stages, however, there is a net outward flow of energy for the case of a liquid and a net inward flow for a gas.

1. Introduction

In the present paper, the investigation of unsteady, viscous flow begun in the paper of Sibulkin (1961*b*), which will be referred to hereafter as Part 1, is continued. In Part 1, results were obtained for an unbounded fluid; in Part 2, the problem of a fluid bounded by a stationary circular cylinder of infinite length and finite radius is considered. The fluid is initially put into two-dimensional, circular motion about the axis of the cylinder, and the subsequent decay of this motion is studied. It is assumed that the cylinder wall is insulated, and our interest will be focused upon the transfer of energy between fluid elements, due to viscous work and heat conduction. The results obtained in this paper will be applied in a later paper to an investigation of the Ranque–Hilsch vortex tube.

The analysis builds upon results obtained in Part 1, and is again limited to flows for which the Mach number is everywhere much less than one. Although it was possible to find solutions in closed form for the case of an unbounded fluid, it has not been possible to do so for the bounded fluid (as might be expected from the similar situation in heat conduction problems; see, for example, Chaps. X and XIV of Carslaw & Jaeger 1959). While the solution of the momentum equation in the form of an infinite series is straightforward, the solution of the energy equation is not. Consequently, the governing equations are converted to finite-difference form and integrated directly. Numerical results for some typical cases are presented and discussed for both liquids and gases. It is hoped that this discussion gives some insight into the mechanism of energy transfer in rotating fluids.

2. Fundamental equations and boundary conditions

In this paper we shall consider two idealized fluids: (i) the *perfect gas* having the equation of state $p = \rho\mathscr{R}T$ and constant values of specific heat c_p and c_v, and (ii) the *perfect liquid* having the equation of state $\rho = \text{const.}$ and a single, constant specific heat c. Hereafter, when the terms gas or liquid are used, they will be understood to refer to the perfect fluids defined above.

When the Mach number satisfies the condition $M \ll 1$ everywhere in the flow field and there is no heat conduction across the boundaries of the fluid, the momentum and energy equations for two-dimensional, axisymmetric flow can be reduced to the form of equations (3.10) and (3.11) in Part 1:

$$\rho r\omega^2 = \frac{\partial p}{\partial r}, \quad \frac{\partial \omega}{\partial t} = \frac{\nu}{r^3}\frac{\partial}{\partial r}\left(r^3\frac{\partial \omega}{\partial r}\right), \tag{1a,b}$$

$$\frac{\partial \Xi}{\partial t} - \frac{\nu}{\sigma r}\frac{\partial}{\partial r}\left(r\frac{\partial \Xi}{\partial r}\right) = \frac{1}{\rho}\frac{\partial p}{\partial t}\delta_{fg} + \frac{\nu}{\sigma r}\frac{\partial}{\partial r}\left[\frac{(\sigma-1)}{2}r^3\frac{\partial \omega^2}{\partial r} - r^2\omega^2\right], \tag{1c}$$

where the momentum equations have been written in terms of the angular velocity ω, and where we have used a general purpose total energy (or enthalpy) variable Ξ and a 'Kronecker δ' defined such that

$$\Xi = H - h_c, \quad \delta_{fg} = 1 \quad \text{(for a gas)}; \qquad \Xi = E - e_c, \quad \delta_{fg} = 0 \quad \text{(for a liquid)}. \tag{1d}$$

In (1*a*) through (1*d*), e and h are the internal energy and enthalpy while E and H are the total energy and total enthalpy; p, ρ, ν, and σ are the fluid pressure, density, kinematic viscosity, and Prandtl number; r and t are the radial and temporal co-ordinates; the subscript c refers to the initial value in the core of the fluid, i.e. the value at $r = 0$, $t = 0$.

For a liquid, changes in pressure do not affect the energy field. For a gas, the increase in enthalpy due to compression of a fluid element can be determined from the radial momentum equation; the result, again for $M \ll 1$ (cf. Part 1, equation (3.9)), is

$$\frac{1}{\rho}\frac{\partial p}{\partial t} = \frac{1}{\rho}\left(\frac{\partial p}{\partial t}\right)_{r=0} + \int_0^r \frac{\partial(\omega^2)}{\partial t} r'\,dr'. \tag{2}$$

The last term in (2) depends only upon the velocity distribution which is determined by the solution of (1*b*) alone; the second term is physically determined by the requirement of conservation of mass

$$\frac{d(\text{mass})}{dt} = 2\pi\int_0^R \frac{\partial \rho}{\partial t} r\,dr = 0, \tag{3}$$

where R is the cylinder radius, and by the equation of state in the differentiated form,

$$\frac{\partial \rho}{\partial t} = \frac{1}{\mathscr{R}}\left[\frac{1}{T}\frac{\partial p}{\partial t} - \frac{p}{T^2}\frac{\partial T}{\partial t}\right], \tag{4}$$

where T is the temperature and $\mathscr{R}$ is the gas constant. Combination of (2), (3) and (4) gives

$$\frac{1}{\rho}\frac{\partial p}{\partial t} = \int_0^1 \left[\left(\frac{\gamma-1}{\gamma}\right)\frac{\partial h}{\partial t} - \int_0^r \frac{\partial(\omega^2)}{\partial t} r'\,dr'\right] d\left(\frac{r}{R}\right)^2 + \int_0^r \frac{\partial(\omega^2)}{\partial t} r'\,dr', \tag{5}$$

where γ is the ratio of specific heats. We define

$$s \equiv r/R, \quad \tau \equiv (\nu/R^2)t, \quad \hat{\omega} \equiv (R/V)\omega, \quad \hat{\Xi} \equiv (2/V^2)\Xi, \quad f \equiv \int_0^s \left(\frac{\partial \hat{\omega}^2}{\partial \tau}\right) s'\,ds', \tag{6}$$

where V is a characteristic velocity, and substitute (6), (5), and (1d) into (1c) and (1b) to give

$$\frac{\partial \hat{\omega}}{\partial \tau} = \frac{1}{s^3}\frac{\partial}{\partial s}\left(s^3 \frac{\partial \hat{\omega}}{\partial s}\right), \tag{7}$$

$$\frac{\partial \hat{\Xi}}{\partial \tau} - \frac{1}{\sigma s}\frac{\partial}{\partial s}\left(s\frac{\partial \hat{\Xi}}{\partial s}\right) = \left[\int_0^1 \left\{\left(\frac{\gamma-1}{\gamma}\right)\left[\frac{\partial \hat{\Xi}}{\partial \tau} - s^2\frac{\partial(\hat{\omega}^2)}{\partial \tau}\right] - 2f\right\} ds^2 + 2f\right]\delta_{fg} + \frac{1}{\sigma s}\frac{\partial}{\partial s}\left[(\sigma-1)s^3\frac{\partial(\hat{\omega}^2)}{\partial s} - 2s^2\hat{\omega}^2\right]. \tag{8}$$

Solving (8) for $\partial\Xi/\partial\tau$ yields

$$\frac{\partial \hat{\Xi}(s,\tau)}{\partial \tau} = g(s,\tau) + \left\{-k(\tau) + \int_0^1 (\gamma-1)\,[g(s,\tau) - k(\tau)]\,ds^2\right\}\delta_{fg}, \tag{9a}$$

where

$$\left.\begin{aligned} g(s,\tau) &\equiv \frac{1}{\sigma s}\frac{\partial}{\partial s}\left(s\frac{\partial \hat{\Xi}}{\partial s}\right) + \frac{1}{\sigma s}\frac{\partial}{\partial s}\left[(\sigma-1)s^3\frac{\partial(\hat{\omega}^2)}{\partial s} - 2s^2\hat{\omega}^2\right] + 2f\delta_{fg}, \\ k(\tau) &\equiv \int_0^1 \left[\left(\frac{\gamma-1}{\gamma}\right)s^2\frac{\partial(\hat{\omega}^2)}{\partial \tau} + 2f\right] ds^2. \end{aligned}\right\} \tag{9b}$$

The momentum and energy equations will be used in the forms given in (7) and (9). The corresponding boundary conditions are

$$\frac{\partial \hat{\omega}}{\partial s}(0,\tau) = 0, \quad \frac{\partial \hat{\Xi}}{\partial s}(0,\tau) = 0, \quad \hat{\omega}(1,\tau) = 0, \quad \frac{\partial \hat{\Xi}}{\partial s}(1,\tau) = 0, \tag{10}$$

where the conditions at $s = 0$ follow from the symmetry of the flow field, and the condition on $\partial\hat{\Xi}/\partial s$ at $s = 1$ follows from the assumption of zero heat transfer across the boundary of the fluid.

For a liquid, the solution of (7), (9) and (10) gives the angular velocity field $\hat{\omega}$ and the total-energy field $\hat{E} \equiv (E - e_c)/\frac{1}{2}V^2$; the circumferential velocity and internal energy fields are then found from

$$\hat{v} \equiv v/V = s\hat{\omega} \quad \text{and} \quad \hat{e} \equiv (e - e_c)/\tfrac{1}{2}V^2 = \hat{E} - \hat{v}^2. \tag{11}$$

For a gas, the solution gives $\hat{\omega}$ and the total enthalpy $\hat{H} \equiv (H - h_c)/\frac{1}{2}V^2$; the total energy and static enthalpy are given by

$$\hat{E} = \hat{H}/\gamma + [(\gamma-1)/\gamma]\hat{v}^2 \quad \text{and} \quad \hat{h} = \hat{H} - \hat{v}^2, \tag{12}$$

while v and e are again given by (11).

3. The density and pressure fields

For a liquid, the density is constant and the pressure is given by integrating (1a) to $p - p_c = \rho\int_0^r \omega^2 r'\,dr'$.

We define

$$\hat{p} \equiv (p - p_c)/\tfrac{1}{2}\rho_c V^2, \quad \hat{\rho} \equiv (\rho - \rho_c)/\mathscr{M}\rho_c; \quad \mathscr{M} \equiv V^2/2h_c = \tfrac{1}{2}(\gamma-1)M^2. \tag{13}$$

The gas law $\rho = [\gamma/(\gamma-1)]\,(p/h)$ can then be written, subject to our limitation to $M \ll 1$, in the non-dimensional form

$$\hat{\rho} = [\gamma/(\gamma-1)]\,\hat{p} - \hat{h}. \tag{14}$$

Since $\hat{h}$ is given in (12), only $\hat{p}$ remains to be determined.

The pressure distribution for a gas, as noted in § 2 during the derivation of $\partial p/\partial t$, depends upon the radial momentum equation, the equation of state, and the conservation of mass. Integrating (1 *a*) and defining

$$F \equiv 2\int_0^s \hat{\omega}^2 s'\,ds' \tag{15a}$$

gives

$$\hat{p}(s,\tau) = \hat{p}(0,\tau) + F(s,\tau). \tag{15b}$$

We combine (14) and (15*b*) with the conservation of mass requirement to give

$$\hat{I}_\rho(\tau) \equiv \pi\int_0^1 \hat{\rho}\,ds^2 = \pi\int_0^1 \{[\gamma/(\gamma-1)]\,[\hat{p}(0,\tau)+F(s,\tau)] - \hat{h}(s,\tau)\}\,ds^2 = \text{const.} \tag{16}$$

By evaluating $\hat{I}_\rho$ at 0 and τ, equation (16) may be solved for $\hat{p}(0,\tau)$; substitution of this result into (15*b*) gives the solution for the gas-flow pressure field as

$$\hat{p}(s,\tau) = F(s,\tau) - \int_0^1 \{F(s,\tau) - [(\gamma-1)/\gamma]\,\hat{h}(s,\tau)\}\,ds^2 + \int_0^1 \{F(s,0) - [(\gamma-1)/\gamma]\,\hat{h}(s,0)\}\,ds^2. \tag{17}$$

In (16) we have defined an integral $\hat{I}_\rho$ which embodies the conservation of mass requirement and is thus invariant with time. Similarly, conservation of energy can be expressed in terms of the integrals

$$\hat{I}_T(\tau) \equiv \pi\int_0^1 (\rho E - \rho_c e_c)\,ds^2 \Big/ \mathscr{M}\rho_c e_c = \text{const.}\dagger \tag{18}$$

and

$$\hat{I}_E(\tau) \equiv \pi\int_0^1 \hat{E}\,ds^2. \tag{19}$$

Since it was shown in equation (7.5) of Part I that $\hat{I}_T$, $\hat{I}_E$, and $\hat{I}_\rho$ are linearly related, it follows that $\hat{I}_E$ must also be invariant with time. These integrals have proved useful in checking the numerical solutions discussed in § 5.3.

4. A finite difference approximation to the equations

The fundamental equations for the decay of an unsteady, viscous, circular flow in a cylinder of finite radius have been given as the pair of linear partial differential equations (7) and (9). The momentum equation (7) is a homogeneous equation which is independent of the energy equation (9). Its solution for an

† This constant value of $\hat{I}_T$ is simpler than the corresponding result given in (7.9) of Part 1 because the finite cylinder considered here is a closed thermodynamic system whereas the infinite fluid in Part 1 was an open thermodynamic system.

arbitrary initial condition, in terms of an infinite series, is straightforward and will be shown in § 5.2. The energy equation, however, is an inhomogeneous equation coupled to the momentum equation; consequently, its inhomogeneous part will involve the infinite-series solution for $\hat{\omega}$. Even if an analytic solution of the energy equation was obtainable, after much effort, in terms of a doubly infinite series, it is doubtful if such a result would provide much insight into the general behaviour of the system. Thus it appeared preferable to attack the fundamental equations directly by means of a finite-difference approximation which would be suitable for machine computation.

The approximation chosen was an explicit difference scheme employing a forward time-difference and central space-differences. The details of the finite-difference analysis are not considered of sufficient interest for presentation here, but are available in Sibulkin (1961*a*). That report includes a discussion of the criteria which must be satisfied to obtain stable solutions of the difference equations, and presents a technique for circumventing an instability in the numerical solutions at the axis of the cylinder which was found to be associated with the singular character of (7) and (9) at $s = 0$.

5. Solutions for a particular flow problem

The fundamental equations and boundary conditions governing circular flows in a stationary cylinder have been given in § 2. In §§ 5.2 and 5.3, solutions of these equations will be presented for the particular set of initial conditions described in the next section.

5.1. *Initial conditions*

The problem which will be solved is that of a circular cylinder of fluid which is initially divided into a quiescent core and an annulus in uniform circular motion, that is

$$v(s,0) = 0 \quad \text{for} \quad 0 \leqslant s < a, \qquad v(s,0) = V \quad \text{for} \quad a < s < 1. \tag{20a}$$

For $s > a$, (20*a*) makes $\hat{\omega}(s,0) = 1/s$. The initial energy distribution chosen to illustrate the energy transfer processes is

$$\hat{E}(s,0) = e_c, \tag{20b}$$

which, by conservation of energy (cf. § 2), can be shown to make $\hat{E}(s,\infty) = e_c$, for both liquids and gases. For a liquid, (20*b*) gives $\hat{\Xi}(s,0) = 0$ for all s; for a gas, using (12), $\hat{\Xi}(s,0) = -(\gamma-1)$ for $s > a$.

5.2. *Series solution for the velocity field*

The general solution of the momentum equation (7) for an arbitrary initial velocity distribution is (McLeod 1922)

$$\hat{v}(s,\tau) = \sum_{i=1}^{\infty} 2\exp(-\lambda_i^2\tau) J_1(\lambda_i s)\,[J_0(\lambda_i)]^{-2} \int_0^1 s^2 \hat{\omega}(s,0)\, J_1(\lambda_i s)\, ds, \tag{21}$$

where the λ_i are the zeros of the Bessel function J_1. (The derivation of (21) is discussed in Part I, § 4.1.) Integration of (21) by parts for the initial condition (20*a*) gives

$$\hat{v}(s,\tau;a) = \sum_{i=1}^{\infty} 2\exp(-\lambda_i^2\tau)\,J_1(\lambda_i s)\,[J_0(\lambda_i)]^{-2} \times\left[(a/\lambda_i)\,J_0(\lambda_i a) - J_0(\lambda_i)/\lambda_i + (1/\lambda_i)^2\int_{\lambda_i a}^{\lambda_i} J_0(\lambda_i s)\,d(\lambda_i s)\right], \qquad (22)$$

where $\int_0^x J_0(t)\,dt$ has been tabulated for $x = 0\,(0{\cdot}01)\,10$ by Lowan & Abramowitz (1943). A comparison of (22) and a finite-difference solution is given later.

5.3. *Finite-difference solutions and discussion of energy-transfer processes*

The finite-difference equations obtained from (7), (9), and (10) together with the initial conditions of § 5.2 were programmed for machine computation. A preliminary survey showed that the value of the parameter a did not change the qualitative character of the results, and the solutions presented in this paper are all for $a = 0{\cdot}6$.

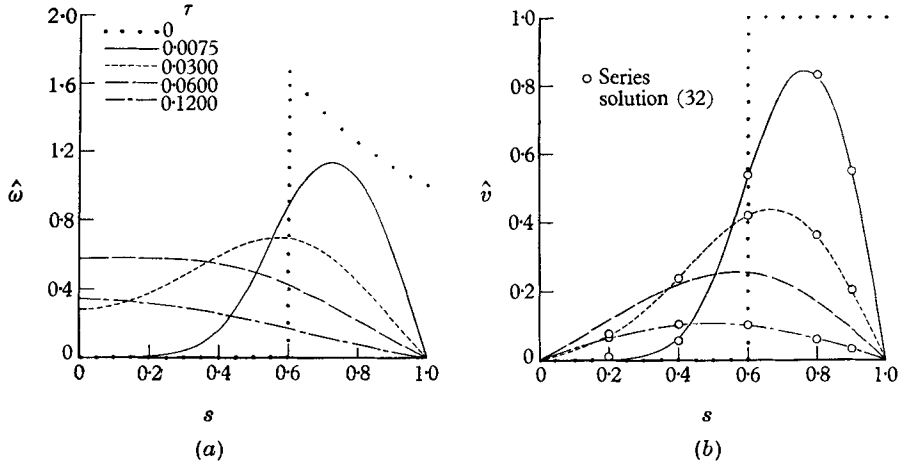

FIGURE 1. Spatial distributions of angular velocity $\hat{\omega} \equiv (R/V)\,\omega$ and circumferential velocity $\hat{v} \equiv v/V$ at successive times $\tau \equiv (\nu/R^2)\,t$.

The angular velocity and circumferential velocity distributions are shown in figure 1. Although the vorticity at the axis of the cylinder is initially zero, it later reaches and remains a maximum there. The early velocity profiles have an inflexion point which is a characteristic of the initial velocity condition (and which will be of interest in the application to the vortex tube). The finite-difference results agree, as they should, with the series solution (22).

In figure 2, typical internal-energy, pressure, and density distributions are shown for a gas having $\gamma = 1{\cdot}4$ and $\sigma = \frac{3}{4}$. (The e profiles, it is clear, are also the static temperature profiles.) For a liquid, the initial distributions of $\hat{e}$ and $\hat{p}$ would be the same; the subsequent $\hat{p}$ profiles would have the same shape as those in figure 2*b*, but with $\hat{p}(0,\tau) = 0$.

For the purpose of discussing the energy transfer processes, it may be useful to write the energy equation (1c) in the form

$$\frac{\partial \Xi}{\partial t} = c_p \frac{\partial T}{\partial t} + \frac{\partial}{\partial t}(\tfrac{1}{2}v^2) = \underset{\text{(i)}}{\frac{1}{\rho}\frac{\partial p}{\partial t}\delta_{fg}} + \underset{\text{(ii)}}{\frac{\nu}{r}\frac{\partial}{\partial r}\left[r^3\frac{\partial}{\partial r}(\tfrac{1}{2}\omega^2)\right]} + \underset{\text{(iii)}}{\frac{k}{\rho r}\frac{\partial}{\partial r}\left(r\frac{\partial T}{\partial r}\right)}, \tag{23}$$

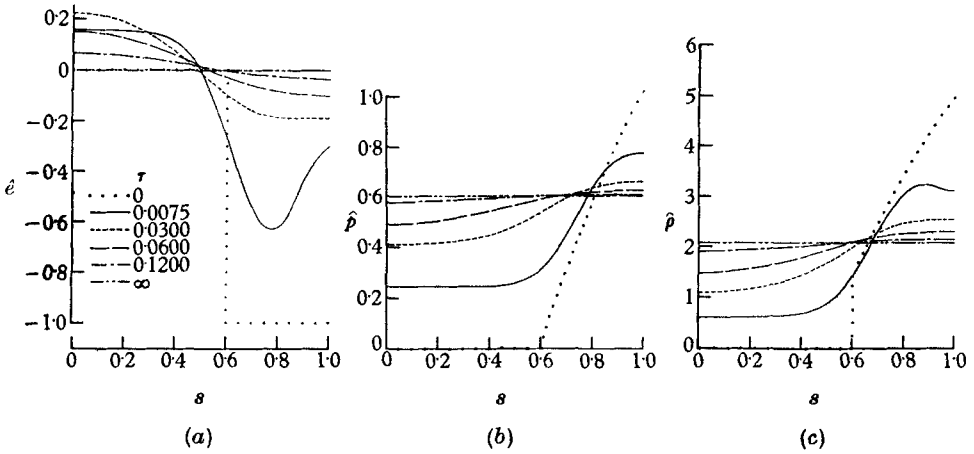

FIGURE 2. Typical internal energy $\hat{e} \equiv (e-e_c)/\frac{1}{2}V^2$, pressure $\hat{p} \equiv (p-p_c)/\frac{1}{2}\rho_c V^2$, and density $\hat{\rho} \equiv (\rho-\rho_c)/\mathscr{M}\rho_c$ distributions for a gas having a ratio of specific heats $\gamma = 1{\cdot}4$ and a Prandtl number $\sigma = \frac{3}{4}$.

where the terms on the right-hand side of the equation represent: (i) the increase in enthalpy due to compression of a fluid element, (ii) the viscous work on an element, and (iii) the net heat conduction into an element. While (i) and (iii) affect only the temperature of a fluid element, the viscous work (ii) affects both its temperature and velocity. This may best be seen by splitting the viscous work term into (cf. Part 1, equation (4.11))

$$\frac{W}{\rho} \equiv \frac{\nu}{r}\frac{\partial}{\partial r}\left[r^3\frac{\partial}{\partial r}(\tfrac{1}{2}\omega^2)\right] = r^2\omega\frac{\nu}{r^3}\frac{\partial}{\partial r}\left(r^3\frac{\partial \omega}{\partial r}\right) + \nu r^2\left(\frac{\partial \omega}{\partial r}\right)^2, \tag{24a}$$

which, by the momentum equation (1b), shows that

$$W = \partial(\tfrac{1}{2}\rho v^2)/\partial t + \Phi, \tag{24b}$$

where Φ is the dissipation function.

In our insulated wall problem, the viscous work acts as a forcing function which alters the initially constant total-energy distribution, while the heat conduction acts as a smoothing function which eventually returns the fluid to a constant-energy condition. With this thought in mind, figure 3 shows the cumulative effect of viscosity and compression on the energy distribution in the absence of heat conduction. For both liquid and gas, the energy of the outermost layer of fluid is increased at the expense of the initial kinetic energy of the remaining fluid in the annulus $s > a$. Viscosity also increases the energy of the fluid just in the interior of $s = a$, by first accelerating this initially quiescent

fluid and then dissipating this acquired kinetic energy into heat. In addition, for a gas, the energy of the fluid interior to $s \approx 0{\cdot}8$ is increased by compression (cf. figure 2*b*) while the energy of the fluid exterior to $s \approx 0{\cdot}8$ is decreased by expansion. Finally, since $v(s,\infty) = 0$ and the energy-transfer processes are continuous across $s = a$, it can be shown that $\hat{E}(a^+,\infty) - \hat{E}(a^-,\infty) = 1$ which is equal to the initial discontinuity in kinetic energy at $s = a$.

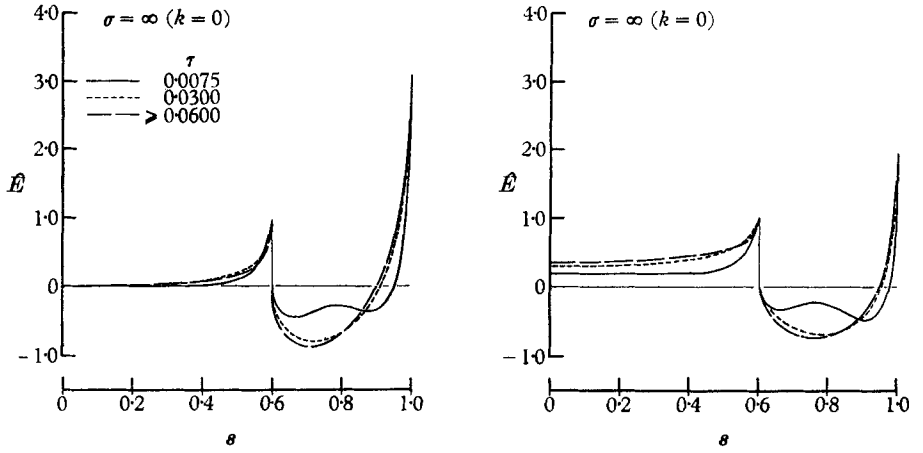

FIGURE 3. Distribution of total energy $\hat{E} \equiv (E - e_c)/\frac{1}{2}V^2$ resulting from the action of viscosity and compression in the absence of heat conduction.

In figure 4, a set of energy distributions at three values of Prandtl number for both a liquid and a gas are presented. The distributions for gases with γ equal to 1·0 and 1·67 did not differ qualitatively from those presented for $\gamma = 1{\cdot}4$. Since the total energy content of the fluid is invariant with time (cf. § 2), $\hat{I}_E(\tau) = \hat{I}_E(0) = 0$ for all the profiles and $\hat{E}(s,\infty) = \hat{E}(s,0) = 0$ since $v(s,\infty) = 0$ and $T(s,\infty) = \text{const}$. The effects of varying the Prandtl number, $\sigma = \mu/(k/c_p)$, can be followed more clearly for the liquid. For $\sigma = \frac{4}{3}$, viscosity predominates at early values of τ and the profiles resemble those for $\sigma = \infty$ (figure 3*a*). For $\sigma = \frac{3}{4}$, thermal conductivity predominates at early values of τ, and the energy profile (especially for $\tau = 0{\cdot}0075$) reflects the heat conduction into the initial static temperature depression at $s > a$ (cf. figure 2*a*). This heat-conduction effect is sufficiently strong, for $\sigma = \frac{3}{4}$, to give a slightly negative value of $\hat{E}$ at $s = 1$, which is reminiscent of the decrease in total temperature at the surface of a plate (recovery factor less than one) which occurs with fluids having similar values of Prandtl number. At later times, however, the liquid energy-profiles for all three Prandtl numbers are similar; the energy increases monotonically from a negative value of $\hat{E}$ at $s = 0$ to a positive value at $s = 1$ showing that there has been a net transfer of energy from the inner to the outer portion of the liquid. The differences between liquid and gas profiles having the same value of σ result primarily from the transfer of energy from the outer to the inner portion of a gas by the work of compression, as discussed in connexion with figure 3.

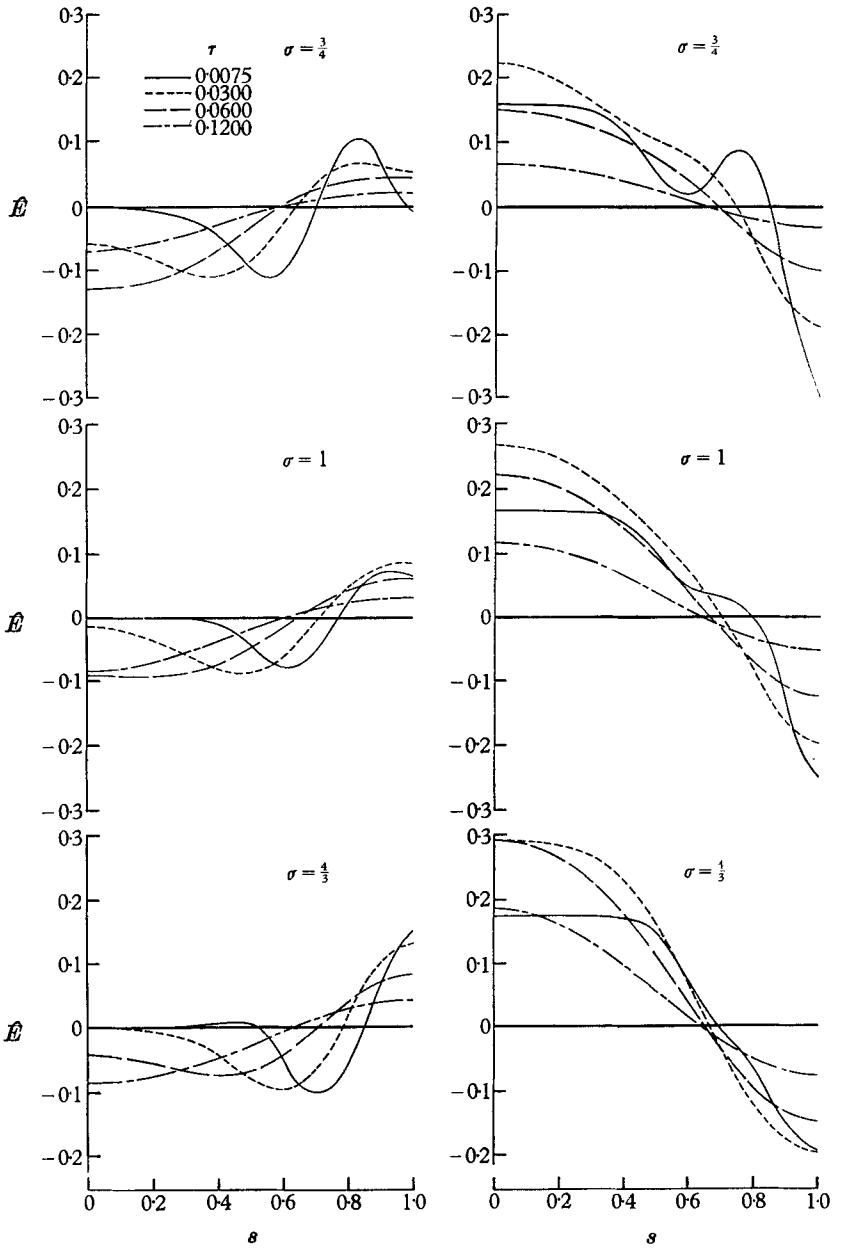

(*a*) Liquid (*b*) Gas, $\gamma = 1{\cdot}4$

FIGURE 4. Comparison of total energy $\hat{E} \equiv (E - e_c)/\frac{1}{2}V^2$ distributions for a liquid and a gas at three values of the Prandtl number σ.

This compression effect is so strong for the gas that, at later times, the energy $\hat{E}$ decreases monotonically from $s = 0$ to $s = 1$, for all three Prandtl numbers.†

For values of $\sigma > \frac{4}{3}$ and $\sigma < \frac{3}{4}$, the liquid energy-profiles have characteristics which are similar to those discussed above. However, as $|\sigma - 1|$ increases, the magnitudes of these energy-transfer effects increase as illustrated in figure 5 where both the maximum and the minimum values of $\hat{E}(s, \tau)$ which occur during the flow process at a particular σ are plotted for values of σ from 0·1 to 10.

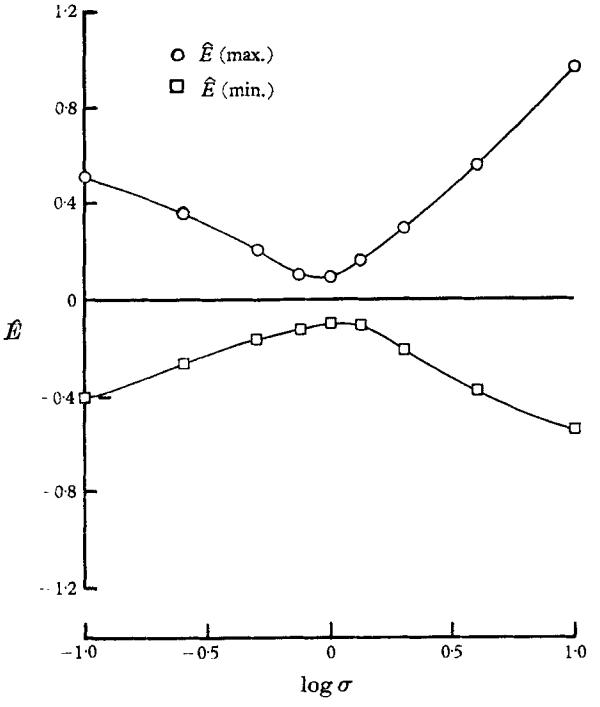

FIGURE 5. Effect of Prandtl number σ on the extrema of the total energy $\hat{E} \equiv (E - e_c)/\frac{1}{2}V^2$ distributions for a liquid.

For $\sigma > 1$, the maxima occur at $s = 1{\cdot}0$ and the minima at $s \approx 0{\cdot}7$; for $\sigma < 1$, the maxima occur at $s \approx 0{\cdot}8$ and the minima at $s \approx 0{\cdot}55$. Figure 5 shows that the maximum value of $|\hat{E}|$ is a minimum for $\log \sigma = 0$, that is, the net energy transfer due to the opposing effects of viscosity and heat conduction is least for $\sigma = 1$. This result for unsteady, viscous, circular flow may be compared with the well-known result that, for steady, viscous, rectilinear flow (boundary-layer flow), the total enthalpy throughout the flow field is constant for $\sigma = 1$.

5.4. *Summary of results*

In conclusion, it may be useful to review the results obtained for the energy-transfer processes in our problem. The assumed uniform initial total-energy distribution (20*b*) is changed by the action of viscosity both by the effect of

† Another interesting example of the difference in energy profiles between liquid and low-speed gas flows having the same velocity field is given by Rott (1959).

viscous shear on the kinetic energy of a fluid element and the effect of viscous dissipation on its internal energy (24). For our circular-flow problem there is an additional indirect effect of viscosity for a gas. The change in the velocity distribution due to shear forces alters the radial pressure distribution which causes the gas elements to expand or contract with an accompanying change in internal energy due to the work of compression (23). For both liquids and gases, the non-uniform temperature distributions, resulting from the assumed initial condition and from viscous dissipation, induce a transfer of energy due to heat conduction which drives the temperature profile towards uniformity (23).

The relative magnitudes of the viscous and heat-conduction effects depend upon the value of the Prandtl number, which strongly affects the spatial distribution of energy during the early stages of the flow (figure 4). During the later stages of the flow, however, the differences in energy distribution due to Prandtl number differences become less pronounced, and we find that there is a net outward flow of energy for the case of a liquid and a net inward flow for a gas. At the conclusion of the flow process the velocity approaches zero due to the action of viscosity, the temperature distribution approaches uniformity due to heat condition, and the energy returns to its uniform initial value as a consequence of conservation of energy.

It is a pleasure to acknowledge the assistance of Mr N. Levine and Mr E. Campbell who programmed the numerical computations.

REFERENCES

CARSLAW, H. S. & JAEGER, J. C. 1959 *Conduction of Heat in Solids*, 2nd ed. Oxford University Press.

LOWAN, A. N. & ABRAMOWITZ, M. 1943 Table of the integrals $\int_0^x J_0(t)\,dt$ and $\int_0^x Y_0(t)\,dt$. *J. Math. Phys.* **22**, 2–7.

MCLEOD, A. R. 1922. The unsteady motion produced in a uniformly rotating cylinder of water by a sudden change in the angular velocity of the boundary. *Phil. Mag.* **44**, 1–14.

ROTT, N. 1959 On the viscous core of a line vortex II. *ZAMP*, **10**, 73–81.

SIBULKIN, M. 1961*a* Unsteady, viscous, circular flow. Part 2. The cylinder of finite radius. *Convair Sci. Res. Lab., San Diego, Res. Note* no. 40.

SIBULKIN, M. 1961*b* Unsteady, viscous, circular flow. Part 1. The line impulse of angular momentum. *J. Fluid Mech.* **11**, 291.